Article

Journal of
Nanoscience and Nanotechnology
Vol. 19, 4270–4275, 2019
www.aspbs.com/jnn

Fabrication of Silver-Doped $(Bi,Sb)_2Te_3$ Thermoelectric Film Prepared from Ag Nanoparticles/Bi–Sb–Te Pastes

Young Min Cho[1,2], Gu Hyun Gwon[1], Soo Hyung Kim[2], Dong Won Kim[1], Jungho Choe[1], and Kyung Tae Kim[1,*]

[1] *Powder Technology Department, Korea Institute of Materials Science, 797 Changwon-daero, Changwon-si, Gyeongnam 51508, Republic of Korea*
[2] *Department of Nano Fusion Engineering, Pusan National University, 1268-50 Samnangjin-ro, Miryang-si, Gyeongnam 50463, Republic of Korea*

Film-type thermoelectric generator (TEG) utilizing Bi–Te based paste has been highly considered as advanced power sources for the wearable electronic devices due to its light, thin and flexible characteristics when producing electricity from certain thermal resources such as human body heat. However, the application of the film-typed TEG has been often limited due to its low TE conversion efficiency caused by low electrical conductivity resulting from severe porosity. Thus, it is crucial to increase electrical properties via densification of the TE film. Here, we synthesized silver nanoparticle (AgNP)-dispersed $(Bi,Sb)_2Te_3$ (BSbT) powders to fabricate AgNP-BSbT pastes by adding organic binder. The synthesized AgNP-BSbT pastes were printed through a hand-painting process and were consolidated into Ag-doped BSbT (Ag-BSbT) thick film with a few hundreds μm with controlled 2-step heat treatment. The microstructures of Ag-BSbT films show abnormally elongated grains but also the amount of porosities in the film significantly decreased by addition of AgNP. As a result, it is confirmed that the 0.072 at% Ag-BSbT thick film exhibits power factor of 2.93×10^{-3} W/mK^2 at room temperature, which is comparable to that of practically utilized bulk materials. It is elucidated that the increase in power factor originates from the modulation between electrical conductivity and Seebeck coefficients due to increased hole carrier density at room temperature.

Keywords: Thermoelectric, Thick Film, Power Factor.

1. INTRODUCTION

A thermoelectric generator (TEG) has attracted much interest as a sustainable and renewable energy source due to its big potential to directly convert thermal energy into electrical energy in solid state. Many researchers have studied on TE materials for improving their energy conversion efficiency, which is determined by dimensionless figure of merit, ZT $(= \alpha^2\sigma T/\kappa)$ where σ is electrical conductivity, α is Seebeck coefficient, κ is thermal conductivity and T is absolute temperature. The simultaneous achievement of increased power factor $(\alpha^2\sigma)$ and reduced κ value is crucial for the improvement of the ZT value. In this regard, lowering κ value has been treated as promising way to increase ZT thus far by making active phonon scattering in the TE materials.[1–3] However, microstructural-control for decrease in thermal conductivity inevitably causes drop in electrical conductivity which results in joule heating due to unavoidable carrier-scattering. In addition, improvement of power factor has not been plausibly achieved due to the trade-off relationship between the Seebeck coefficient and the electric conductivity, which are mainly influenced by carrier concentration.[4]

In the case of the TEG fabricated with the TE polymers, the improvement in the power factors is also crucial because polymers, currently available in flexible TE devices, exhibit low TE properties. Polymer-based TE materials such as poly(3, stroll4-ethylenedioxythiophene) (PEDOT) and PEDOT:poly(styrenesulfonate) (PSS) have many benefits when these are applied to curved surfaces and wearable devices due to their excellent flexibility and low intrinsic thermal conductivity.[5–9] Recently, Cho et al. reports the high power factor of 284 μWm^{-1}K^{-2}

*Author to whom correspondence should be addressed.

1533-4880/2019/19/4270/006 doi:10.1166/jnn.2019.16271

which is achieved from Te-PEDOT:PSS composite, but the value is still insufficient for practical usage compared to that of conventional bulk Bi–Te based alloys which are commercially used in many applications.[10]

Thus, printing processes using inorganic materials-based TE ink or paste is considered to be an alternative method to produce the flexible TE generator instead of utilizing polymer-based TE materials.[11] For the printing process, TE paste composed of inorganic TE materials such as Bi–Te alloy and organic binder is required. However, thin film made of TE materials results in lower ZT values than expected due to their poor electrical conductivity caused by incomplete heat treatment conditions and an ineffective removal of polymer binders in the inorganic paste/ink.[12]

Several researchers reported advanced heating techniques such as a post ionized defect engineering method by controlling the forming gas during the heat treatment on the screen printed film. Cho et al. confirms the maximum ZT of 0.9 which is obtained from *n*-type $Bi_2Te_{2.7}Se_{0.3}$ thick film at room temperature.[13] However, the TE films fabricated through the aforementioned post ionized defect process results in a low relative density which implies high porosity level. Therefore, the electrical properties have shown insufficient values than that of commercial Bi–Te based TE materials.[14] As such, there has been rarely studied on specific heat treatment for the highly densified TE film but also the results in comparable power factor value to that of bulk materials has not been reported in printed thick film system.

In this study, we synthesize the silver nanoparticle (AgNP)-dispersed $Bi_{0.5}Sb_{1.5}$–Te_3 (AgNP/BSbT) powders for hand painting process with TE paste that can be utilized as an alternative process to the screen printing. Since silver (Ag) is well known as a p-type dopant in BSbT materials, the addition of AgNP is expected to provide affirmative effect in electrical conductivity by increasing carrier density (n) in BSbT film.[15] Therefore, the developed paste of the Ag/BSbT material incorporated with organic binders is painted and then solidified as the film through 2-step heat treatment that was conducted to achieve highly densified sample of Ag-doped BSbT (Ag-BSbT) film. The 2-step heat treatment not only effectively removes the solvent and the binder in the TE paste but also induces grain growth in the TE films, thereby minimizing the pores present inside the film.

2. EXPERIMENTAL PROCEDURE

The fabrication process of Ag-BSbT film was sequentially displayed in photos of Figure 1(a). Raw materials of bismuth, antimony and tellurium purchased from (Materion Co. Ltd., USA) was directly milled by high energy ball milling process (Fritsch Monomill, Pulverisette, Germany) into $Bi_{0.5}Sb_{1.5}Te_3$ powders under 450 rpm for 11 hr. The Ag nanoparticles were prepared by the Tollen's method;[16] silver nanoparticles are produced by the redox action of silver ammonia complex and glucose-embedded solution, and the silver ammonia complex is formed by the oxidation-reduction reaction of ammonia solution and silver oxide which is synthesized by redox reaction with Silver nitrate ($AgNo_3$) and Sodium hydroxide diluted in distilled water. The fabricated BSbT powder was mixed with the synthesized AgNP by the contents of Ag, which are 0.072 at%, 0.144 at%, 0.287 at%, 0.567 at% and 1.127 at%, and then organic binders, which are composed of ethyl cellulose and α-terpineol, were homogeneously added to prepare a TE paste. Each TE paste was painted in the form of a film which is 10×10 mm in width and a few hundreds of μm in thickness on the alumina substrate through a hand painting. Heat treatment for the printed films were conducted under 2 step-sintering at 60 °C for 24 hours under 0.2 Bar with vacuum oven and at 450 °C for 6 hours in hydrogen gas atmosphere, respectively. The first step is mainly for removing organic binders from the BSbT pastes and rearranging TE powders. The second step is designed for not only high temperature sintering but also densification of TE film. The phases of the powders and fabricated films were characterized by the X-ray diffraction method (Rigaku., D/MAX 2500, JAPAN) and the surface microstructures of the powders and films were analyzed by scanning electron microscopy (SEM, Jeol 5800 LV). Hall measurement system (Ecopia, Model AHT55T3, South Korea) and Seebeck coefficient measurement system were used to evaluate the electrical properties of the fabricated TE films.

3. RESULTS AND DISCUSSION

Figure 1(b) shows XRD patterns of BSbT Powder synthesized by high energy ball milling process of raw materials. The patterns correspond to $Bi_{0.5}Sb_{1.5}Te_3$ phase matched with JCPDS PDF no. 19-1713. The inset SEM image shows that the powder shows few micrometers in average powder sizes. As shown in Figure 1(c), the XRD patterns and inset SEM image of the Ag nanoparticles synthesized by Tollen's method indicates clear silver phase and 400 nm in average size, respectively. It is observed that the cross sectional SEM image of BSbT film has very uniformly formed on the substrate and its thickness is measured as approximately 400 μm as shown in Figure 1(d). The energy dispersive X-ray spectroscopy (EDS) displayed in Figure 1(d) exhibits that the Bi, Sb and Te atoms in the film are homogeneously alloyed rather than randomly concentrated.

Figures 2(a)–(f) show the microstructures of fabricated TE films changed by addition of AgNP; paintable BSbT pastes which is the mixture of $Bi_{0.5}Sb_{1.5}Te_3$ powder, AgNP and organic binder we produced were painted onto the alumina substrate via hand-printing and the pastes were heated in the furnaces by 2 step heating treatment. Figure 2(a) shows a surface microstructure of BSbT film

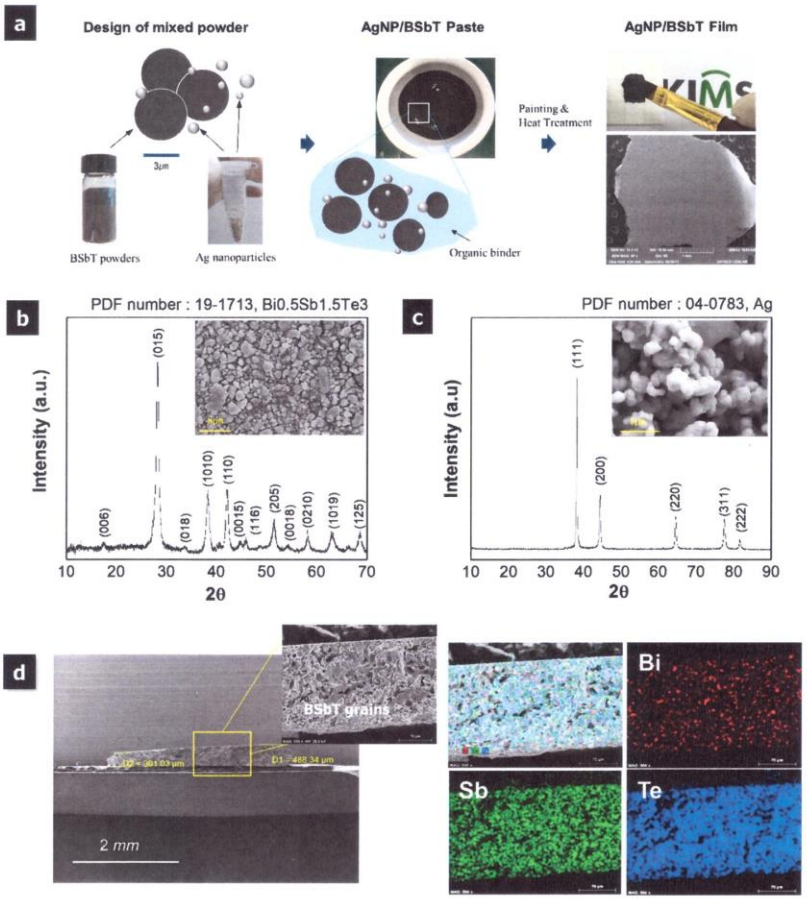

Figure 1. (a) Schematic diagrams of producing the TE film. XRD patterns and SEM image of (b) BSbT composite powders and (c) fabricated Ag nanoparticles. (d) SEM images and the EDS results of cross sectional BSbT film.

fabricated by the same process without any AgNP for confirmation of effects by Ag doping. The grain size of the BSbT film appears to be slightly larger than the size of the powder, and the powder is connected to each other to form a network by active atom-diffusion as temperature increases. The SEM images of Figures 2(b)–(f) shows surface morphologies of Ag-BSbT films where the concentration of Ag is controlled as the 0.072 at%, 0.144 at%, 0.287 at%, 0.567 at%, and 1.127 at%. Interestingly, it is observed that the grain size of BSbT films has become larger and the shape of grain was significantly elongated when AgNP is added. The elongated grain might be abnormally grown during heat treatment due to the presence of Ag atoms that hinder grain boundary migration in the BSbT film. Figure 2(g) shows XRD patterns of the Ag-BSbT film compared to those of BSbT powder and film. The phase of BSbT is consistently remained even after heat treatment to the powders. All of patterns match well with JCPDS card no. 19-1713, which corresponds to the phase of $Bi_{0.5}Sb_{1.5}Te_3$. The XRD patterns of the BSbT film generally demonstrates that the intensity of the peak corresponding to plane (015) is much sharply higher than those of others, but there are different features in the case of each Ag-BSbT films; although the intensity of the peak corresponding to plane (015) is still the highest in every TE film, the intensity in the 0.144 at% Ag-BSbT is significantly reduced and similar to other peaks. This means that there are no big differences in crystallinity among the films but also any secondary phases does not present.

The average grain size of the Ag-BSbT film was displayed as a function of contents of Ag in Figure 2(h). The grain size is calculated from method of mean linear intercept $\bar{l}$.[17] With the relationship between the number of grains per unit (N_v) and $\bar{l}$ via the mean liner intercept method, the average grain size, $\bar{D}$,

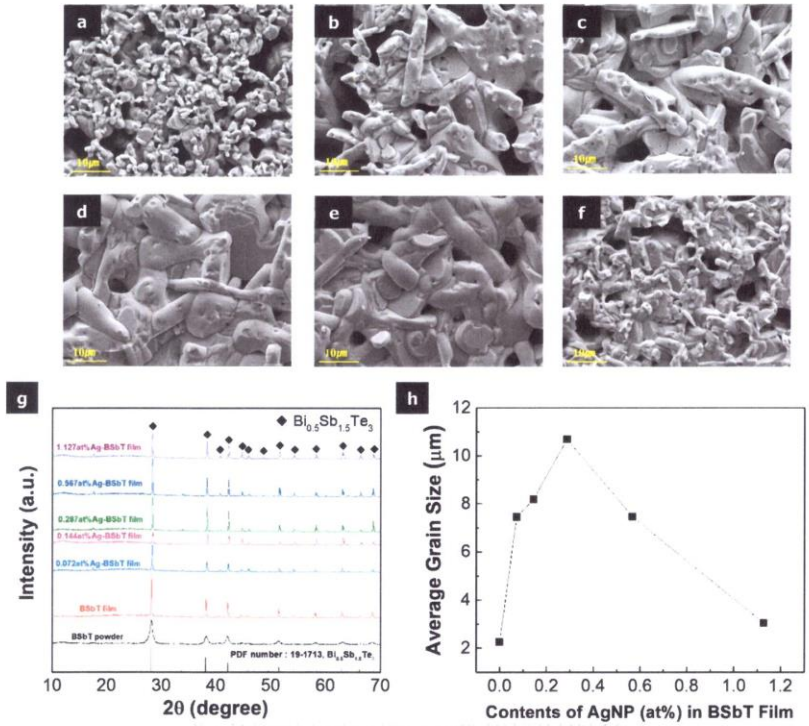

Figure 2. Microstructures of (a) BSbT film, (b) 0.072 at% Ag-BSbT film, (c) 0.144 at% Ag-BSbT film, (d) 0.287 at% Ag-BSbT film, (e) 0.567 at% Ag-BSbT film, (f) 1.127 at% Ag-BSbT film. (g) XRD patterns of BSbT powder and all fabricated TE films (h) average grain size of all fabricated TE films.

was calculated by

$$\bar{D} = 1.7756(\exp^{-2.5\ln^2 S})\bar{l} \quad (1)$$

where S is the standard deviation of the log-normal distribution. According to the graph, the 0.287 at% Ag-BSbT film shows the largest grain among them and the film doped with more than the 0.287 at% of Ag has grains which become smaller as the degree of doping increases. The most notable point is that the porosity of all Ag-BSbT films have significantly been decreased. This tendency in density leads to improvement of electrical properties in the BSbT films.

Figure 3(a) shows variation of carrier density (n) and the carrier mobility (μ) in the Ag-BSbT films. The carrier density increases as the Ag content increases, and the peak carrier density reaches to 2.65×10^{20} cm^{-3} when the 1.127 at% Ag is doped to the BSbT film. But the carrier mobility decreases ranging from 129 to 43 $cm^2V^{-1}S^{-1}$ as the Ag content increases. Figure 3(b) shows the electrical conductivity (σ) and the Seebeck coefficient (α) of BSbT films varied with contents of Ag. The relationship between electric conductivity and Seebeck coefficient can be expressed as following equations:

$$\sigma = ne\mu \quad (2)$$

$$\alpha = \frac{8\pi^2 k_B^2}{3eh^2} m^* T \left(\frac{\pi}{3n}\right)^{2/3} \quad (3)$$

where n, μ, k_B, h, m^* are carrier density, carrier mobility, Boltzman constant, Planck constant and effective mass, respectively. According to the Eqs. (2) and (3), although electrical conductivity depends on carrier density and mobility, the Seebeck coefficient have inverse relationship with carrier density and is up to the change of the effective mass; that is as the carrier density increases, the Seebeck coefficient decreases. As the carrier density increases, electrical conductivity increases up to 20.25×10^4 S/m at the 0.567 at% Ag-BSbT film. The Seebeck coefficient decreases as the Ag content increases, when compared to peak value, 255 μV/K obtained from the BSbT film without AgNP. As shown in Figure 3(c), the pisarenko plot of the Seebeck coefficient as a function of carrier density shows that the effective mass (m^*) of the 0.072 at% Ag-BSbT film is 1.29 times heavy mass of the hole compared to rm^* values of other films. This graph indicates

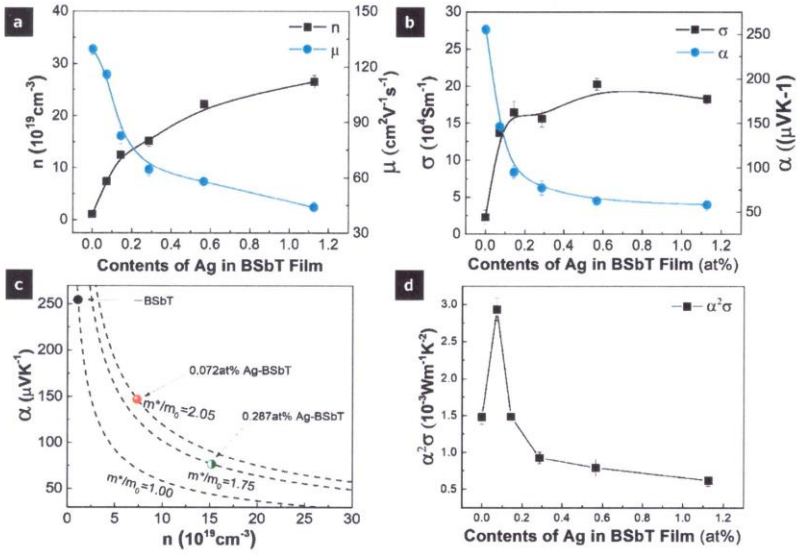

Figure 3. (a) Carrier density and mobility, (b) electrical conductivity of BSbT film as a function of contents of Ag, (c) pisarenko plot showing relationship between Seebeck coefficient and carrier density and (d) comparison of power factor values with contents of Ag.

why the 0.072 at% Ag-BSbT film shows high Seebeck coefficient despite the same carrier density as other films. Figure 3(d) shows the power factor ($\alpha^2\sigma$) changes of the TE films with contents of AgNP. Densified microstructures in TE films have a positive effect on increase in electrical conductivity. However, the electrical conductivity of 0.287 at% Ag-BSbT, which shows the lowest porosity, is similar to those of the 0.072 and 0.144 at% Ag-BSbT films, respectively. It is analyzed that carrier scattering by the Ag doping has more influence on decrease in a carrier mobility rather than the increase of carrier density. In addition, as the peak of the 015 plane decreases with the densification of the TE film with adding AgNP, the drop in the mobility is caused by the decrease of the anisotropic crystallinity of the BSbT. As a result, the power factor has a value of 1.48×10^{-3} W/mK^2 for the film when AgNP is not added, and about 2.93×10^{-3} W/mK^2 which is the highest power factor records with the 0.072 at% Ag content. When the Ag is doped more than the 0.072 at%, the power factor gradually decreases due to the significantly lower Seebeck coefficient compared to the small increase in electrical conductivity. Therefore, the main factor for the increase of the power factor is the optimization of the electrical conductivity, Seebeck coefficient by adjusting the carrier density and effective mass through AgNP addition, and it is considered that the abnormal grain growth and the increased density due to addition of Ag also additionally acted.

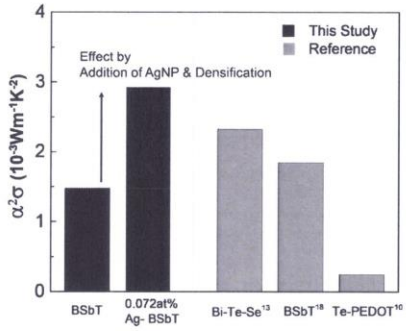

Figure 4. Power factor values of a BSbT and a Ag-BSbT film compared with that of other studies.[10, 13, 18]

4. CONCLUSION

The paintable TE paste was synthesized by mixing AgNP and BSbT powders and they were consolidated into the highly densified thermoelectric thick-film through a controlled heat-treatment. It is confirmed that the developed painting process using the paste can be effectively replaced for screen printing method but also it produces high-performance Ag-BSbT thick film. In addition, it was confirmed that 2-step heat treatment we developed makes it effective to remove the organic binder in BSbT paste and densify the fabricated TE films at the same time. As a result, it was firstly observed that grain growth of BSbT grains actively occurs in the film by addition of AgNP and shape of the grains has become elongated during the 2 step heat treatment process on the substrate. The peak power factor, which records 2.93×10^{-3} W/mK^2 in the 0.072 at%

Ag-BSbT film, shows approximately 2 times higher than 1.48×10^{-3} W/mK^2 of BSbT film without AgNP. This result shows the greatest power factor among the TE films prepared from the Bi–Te paste and it is about 10 times higher than that of the TE polymer (Fig. 4). That can be described that the Ag in the films affects increase of hole carrier density in *p*-type BSbT materials as well as achievement in high relative density. Hence, these results clarify that our processes and TE materials can be utilized for making high-performance *p*-type TE thick films.

Acknowledgment: This work was supported by a grant (Code No. NRF2014M3A6B3-063704) from the Global Frontier Research Program of the Ministry of Science, ICT and Future Planning of the Republic of Korea and Kyung Tae Kim thanks to the Core Research Project on Nano-Materials (Code No. 2016M3A7B4900) funded by National Research Foundation of the Republic of Korea.

References and Notes

1. A. I. Hochbaum, R. Chen, R. D. Delgado, W. Liang, E. C. Garnett, M. Najarian, A. Majumdar, and P. Yang, *Nature* 451, 163 (**2008**).
2. K. T. Kim, S. Y. Choi, E. H. Shin, K. S. Moon, H. Y. Koo, G. G. Lee, and G. H. Ha, *Carbon* 52, 541 (**2013**).
3. K. T. Kim, T. S. Min, and D. W. Kim, *J. Kor. Powd. Met. Inst.* 23, 263 (**2016**).
4. G. J. Snyder and E. S. Toberer, *Nat. Mater.* 7, 105 (**2008**).
5. O. Bubnova and X. Crispin, *Energy Environ. Sci.* 5, 9345 (**2012**).
6. D. S. Maddison, J. Unsworth, and R. B. Roberts, *Synth. Met.* 26, 99 (**1988**).
7. F. Yakuphanoglu and B. F. Şenkal, *J. Phys. Chem. C* 111, 1840 (**2007**).
8. I. Lévesque, P.-O. Bertrand, N. Blouin, M. Leclerc, S. Zecchin, G. Zotti, C. I. Ratcliffe, D. D. Klug, X. Gao, F. Gao, and J. S. Tse, *Chem. Meter.* 19, 2128 (**2007**).
9. Q. Wei, M. Mukaida, K. Kirihara, Y. Naitoh, and T. Ishida, *Appl. Phys. Express* 7, 031601 (**2014**).
10. E. J. Bae, Y. H. Kang, K.-S. Jang, and S. Y. Cho, *Scientific Reports* 6, 18805 (**2016**).
11. Z. Lu, M. Layani, X. Zhao, L. P. Tan, T. Sun, S. Fan, Q. Yan, S. Magdassi, and H. H. Hng, *Small* 10, 3551 (**2014**).
12. C. Navone, S. Plissonnier, and A. L. Seiler. *J. Electron Mater.* 39, 1755 (**2010**).
13. S. J. Kim, H. Choi, Y. Kim, J. H. We, J. S. Shin, H. E. Lee, M.-W. Oh, K. J. Lee, and B. J. Cho, *Nano Energy* 31, 258 (**2017**).
14. K. Hiraishi, A. Masuhara, H. Nakanishi, H. Oikawa, and Y. Shinohara, *Jpn. J. Appl. Phys.* 48, 071501 (**2009**).
15. J. Horák, P. Lošťák, L. Šiška, and M. Stordeur, *Phys. Status Solidi B* 114, 39 (**1982**).
16. Y. Yin, Z.-Y. Li, Z. Zhong, B. Gates, Y. Xi, and S. Venkateswaran, *J. Mater. Chem.* 12, 522 (**2002**).
17. M. I. Mendelson, *J. Am. Ceram. Soc.* 52, 443 (**1967**).
18. S. H. Park, S. Jo, B. Kwon, F. Kim, H. W. Ban, J. E. Lee, D. H. Gu, S. H. Lee, Y. Hwang, J.-S. Kim, D.-B. Hyun, S. Lee, K. J. Choi, W. Jo, and J. S. Son, *Nat. Commun.* 7, 13403 (**2016**).

Received: 29 December 2017. Accepted: 27 February 2018.